Available online at www.sciencedirect.com
ScienceDirect
Tetrahedron: Asymmetry
Tetrahedron: *Asymmetry* 18 (2007) 1448–1456

Stereoselective synthesis and conformational analysis of pseudo-heptapeptides: Part 5☆

Daniele Balducci, Andrea Bottoni, Matteo Calvaresi, Gianni Porzi* and Sergio Sandri*

Dipartimento di Chimica 'G.Ciamician', Università di Bologna, Via Selmi 2, 40126 Bologna, Italy

Received 8 May 2007; accepted 14 June 2007

Abstract—The stereoselective synthesis of pseudo-heptapeptides **8**, **9** and **12**, incorporating a 2,6-diamino-4-methylen-1,7-heptanedioic acid residue, was accomplished starting from chiral synthon **3**, a masked unnatural dipeptide derived from an L-valine unit and (2*R*)-methylaspartic acid. Investigations of the conformational preference and structure of these unnatural peptides were carried out using ^{1}H NMR and IR spectroscopic data and a conformational analysis based on molecular dynamics (MD).

1. Introduction

Recently we described the stereoselective synthesis of unnatural tri-peptides incorporating an α,α′-diamino-dicarboxylic structure mimetic of 2,6-diaminopimelic acid.[1–5] In particular, we reported the synthesis of six pseudo-tetrapeptides containing two L-valine units and two modified α-amino acids such as proline and aspartic acid.[5] The conformational analysis performed on these pseudo-peptides showed the existence of intra-molecular hydrogen bonds (between the carbonyl oxygen atoms and amide protons) responsible for the formation of β- and γ-folded conformers. Therein, we reported that ^{1}H NMR and IR data, coupled to a conformational analysis based on molecular dynamics, are a valid tool to elucidate the structures of unnatural peptides.[5]

Herein we report a further application of our simple protocol to synthesize new pseudo-heptapeptides, starting from chiral synthon **1** (a monolactim ether, see Scheme 1), which can be easily obtained from L-valine.[6] We were interested in the synthesis of new and more complex pseudo-peptides because in previous stereoselective approaches[1,3,4] to non-classical tri-peptides incorporating the γ-methylene derivative of 2,6-diaminopimelic acid, we observed the formation of intra-molecular hydrogen bonds, responsible for the formation of compact symmetrical 'U shaped' conformations. Herein we decided to continue along this research line. Thus, we have synthesized new and more complex pseudo-peptides incorporating the γ-methylene derivative of 2,6-diaminopimelic acid. Our purpose was to verify, in this molecular framework, the presence of intra-molecular hydrogen bonds, which could determine the formation of compact structures, such as a β- or γ-reverse turn, similarly to that previously observed.[1,3,4]

2. Synthesis

The more complex unnatural heptapeptides **8**, **9** and **12** (see Schemes 1 and 2) were obtained using chiral synthon **3**[7a] [a masked cyclic pseudo-dipeptide derived from an L-valine unit and (2*R*)-methylaspartic acid] and following the previously described procedure.[1–4] The synthesis is based on the property of chiral synthon **2**, which can act as an electrophile (see Ref. 7). The masked unnatural heptapeptides **6** and **7** were obtained in good to satisfactory yields, respectively, by coupling acid **3** with the γ-methylene derivative of 2,6-diaminopimelic acid **4** or **5**,[1] in the presence of 4-(4,6-dimethoxy-1,3,5-triazin-2-yl)-4-methylmorpholinium chloride (DMTMM)[8] (see Scheme 1).

We observed that the coupling reaction of chiral synthon **3** with **5** was considerably slower than that involving species **4**. The subsequent acid hydrolysis was carried out under mild conditions, while the following treatment with acetyl chloride allowed us to afford in satisfactory yield the pseudo-heptapeptides **8** and **9**, containing four L-valine units

☆ Refs. 1–4 are considered to be Parts 1–4, respectively.

* Corresponding authors. E-mail: gianni.porzi@unibo.it

0957-4166/$ - see front matter © 2007 Elsevier Ltd. All rights reserved.
doi:10.1016/j.tetasy.2007.06.016

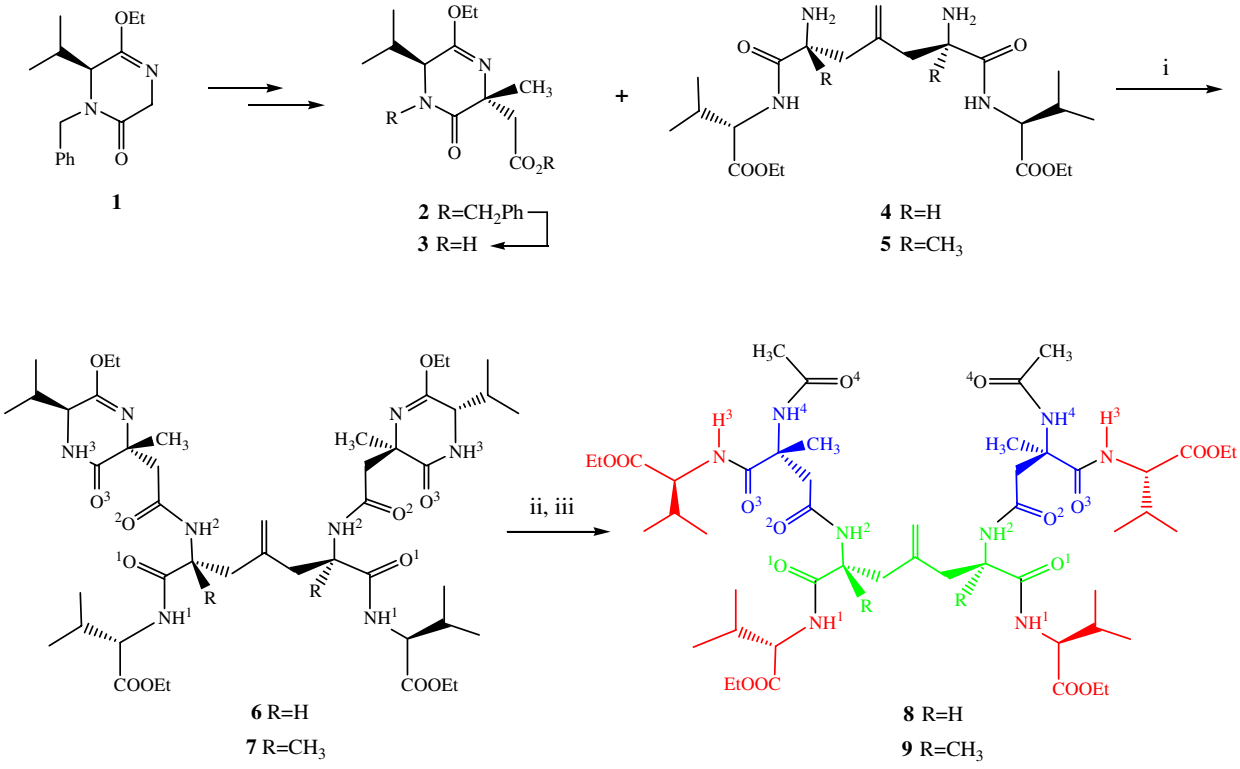

Scheme 1. Reagents and conditions: (i) **3** in the presence of DMTMM in THF at rt; (ii) 0.5 M HCl in EtOH; (iii) CH_3COCl in CH_2Cl_2 in the presence of Et_3N.

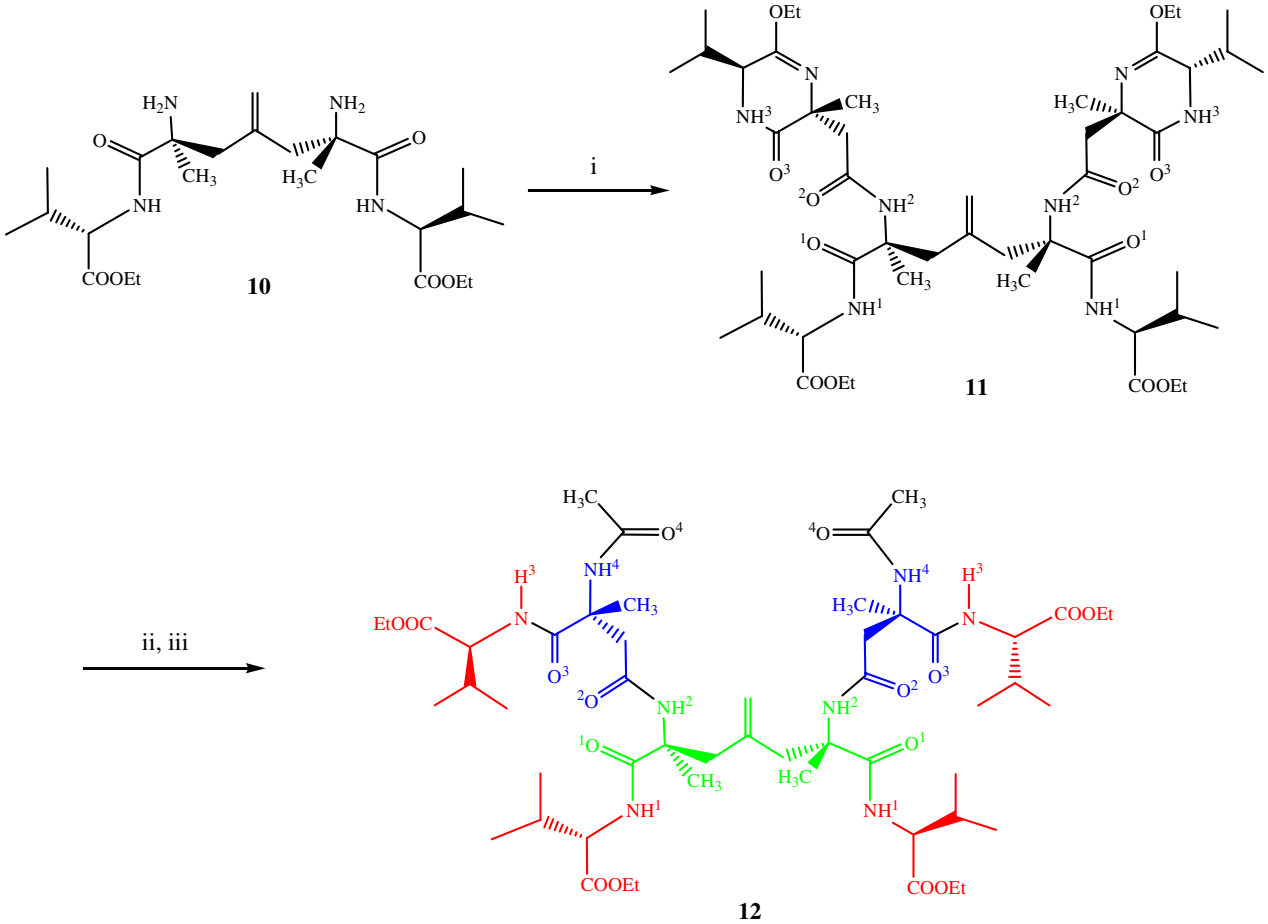

Scheme 2. Reagents and conditions: (i) **3** in the presence of DMTMM in THF at rt; (ii) 0.5 M HCl in EtOH; (iii) CH_3COCl in CH_2Cl_2 in the presence of Et_3N.

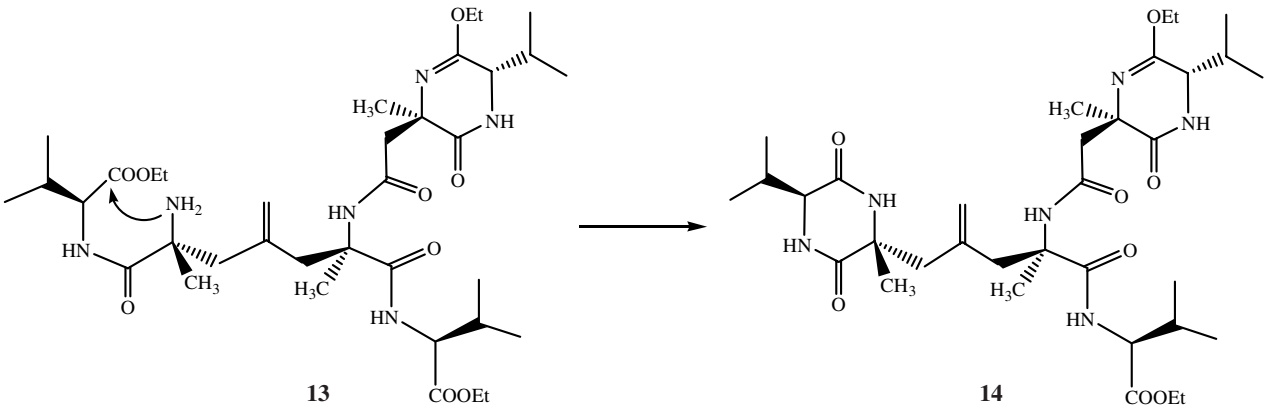

Scheme 3.

(red), two modified aspartic acid units (blue) and the γ-methylene derivative of 2,6-diaminopimelic acid (green). These unnatural peptides contain four pairs of amidic NH groups that can originate hydrogen bonds with the carbonyl oxygen atoms.

We were able to synthesize the masked pseudo-heptapeptide **11** (diastereomer of **7**) using a similar procedure, by coupling chiral synthon **3** with the γ-methylene derivative of 2,6-diaminopimelic acid **10**[1] (Scheme 2).

In this case, the coupling reaction between electrophile **3** and nucleophile **10** was remarkably slower than the corresponding reactions involving nucleophile **4** or **5** and occurred in moderate yield. This result can be understood if we consider that, in addition to pseudo-heptapeptide **12**, diketopiperazine **14** was formed from the monoacyl intermediate **13**. This product is due to the intra-molecular nucleophilic attack of amine group on the ester function of the L-valine residue (Scheme 3). Intermediate **13** and product **14** were recognized by HPLC–MS.

Thus, the coupling reaction appears to be affected either by the steric hindrance or by the configuration of the stereocentre adjacent to the amine group.

The pseudo-heptapeptide **12** (a diastereomer of **9**) was achieved in satisfactory yield after hydrolysis of intermediate **11** and subsequent acetylation (see Scheme 2).

3. ^{1}H NMR and IR studies

Spectroscopic ^{1}H NMR and IR studies were carried out in order to investigate the structural features of pseudo-heptapeptides **8**, **9**, **12** and their precursors **6**, **7**, **11**. As observed in the previous papers,[3,4] and in the present case as well, the ^{1}H NMR spectra of these 'non-classical pseudo-peptides' (**6**, **7**, **8**, **9**, **11**, **12**) indicate the presence of a C_2-symmetry axis. This symmetry element is evidenced by the overlap of the signals of both *iso*-propyl groups. The same behaviour was observed for the signals of the methyl, methylene, methine groups and the amide hydrogen atoms (see Section 6), these nuclei being chemical shift equivalent (i.e., magnetically equivalent). In addition, the chemical shift of the NH amide protons does not display concentration dependence, suggesting that these structures, at least at the concentration investigated here, do not form intermolecular aggregates.

The existence of hydrogen bonds was inferred from the amide proton chemical shift (δ_{NH}), which changed upon the addition of 20% DMSO, and the value of the temperature coefficient ($\Delta\delta_{NH}/\Delta T$),[1–5] although this parameter is not always a key-factor for establishing the formation of

Table 1. Relevant ^{1}H NMR parameters and IR data for substrates **6**–**9**, **11** and **12**

	δ_{NH} (ppm)[a]	δ_{NH} (ppm)[b]	$\lvert\Delta\delta_{NH}/\Delta T\rvert$ (ppb/°C)[a]	IR (cm^{-1})[c]
6	**H^1** 7.52 (d)	**H^1** 7.70	**H^1** 2.6	3275, 3315, 3404
	H^2 7.74 (d)	**H^2** 8.26	**H^2** 3.0	
	H^3 7.47 (s)	**H^3** 7.60	**H^3** 6.0	
7	**H^1** 7.59 (d)	**H^1** 7.67	**H^1** 3.3	3306, 3366, 3400
	H^2 6.89 (s)	**H^2** 7.14	**H^2** 1.6	
	H^3 6.96 (s)	**H^3** 7.27	**H^3** 4.0	
8	**H^1** 7.22 (d)	**H^1** 7.83	**H^1** 3.3	3317, 3420
	H^2 7.54 (d)	**H^2** 7.80	**H^2** 3.3	
	H^3 7.95 (d)	**H^3** 7.77	**H^3** 0.6	
	H^4 7.68 (s)	**H^4** 7.86	**H^4** 1.7	
9	**H^1** 7.63 (d)	**H^1** 7.68	**H^1** 3.7	3267, 3366, 3426
	H^2 7.45 (s)	**H^2** 7.80	**H^2** 1.1	
	H^3 7.99 (d)	**H^3** 8.13	**H^3** 0.2	
	H^4 7.58 (s)	**H^4** 7.92	**H^4** 1.3	
11	**H^1** 7.79 (d)	**H^1** 7.78	**H^1** 3.1	3369, 3434[d]
	H^2 7.08 (s)	**H^2** 7.37	**H^2** 1.0	
	H^3 6.34 (s)	**H^3** 7.08	**H^3** 0.9	
12	**H^1** 8.00 (d)	**H^1** 7.86	**H^1** 4.3	3358, 3437[e]
	H^2 7.40 (s)	**H^2** 7.43	**H^2** 1.7	
	H^3 8.50 (d)	**H^3** 7.97	**H^3** 4.8	
	H^4 7.76 (s)	**H^4** 7.82	**H^4** 1.2	

[a] 2 mM solution in $CDCl_3$; the multiplicity of the signal is reported in parentheses.
[b] In $CDCl_3$ + 20% DMSO.
[c] 2 mM solution in $CHCl_3$.
[d] Weak band.
[e] Shoulder.

hydrogen bonds, particularly in cross-linked peptides.[9] Useful information can also be attained from the infrared spectra in dilute solution: a broad band in the range 3300–3370 cm^{-1} indicates the presence of an intra-molecular hydrogen bond, while a sharp band higher than 3400 cm^{-1} is representative of a free amidic NH stretching.

The significant ^1H NMR parameters and IR absorptions obtained for the various substrates in diluted solution are collected in Table 1. Here the amide protons are labeled as $\mathbf{H^1}$, $\mathbf{H^2}$, $\mathbf{H^3}$ or $\mathbf{H^4}$ (see Schemes 1 and 2).

The ^1H NMR spectra assignments of the amide protons were decided on the basis of the signal multiplicity as well as by irradiation and/or NOE measurements. First of all, it is important to underline that, as already observed, the NH proton in the monolactim ethers appears as a quasi-broad singlet.[1,7] The NH^1 and NH^2 doublets in pseudo-peptide **6** were distinguished by spin–spin decoupling. In fact, irradiating the $\underline{H}C–NH^1$ (dd at 4.47 ppm) the NH^1 doublet at 7.52 ppm collapses to a singlet and by irradiation of $\underline{H}C–NH^2$ (the multiplet at 4.67 ppm) the NH^2 signal was simplified to a singlet. In pseudo-peptide **8**, the doublet at 7.54 ppm was unequivocally assigned to the NH^2 proton since this signal becomes a singlet by irradiating the multiplet at 4.71 ppm ($\underline{H}C–NH^2$). The assignment of NH^1 and NH^3 doublets was instead achieved by NOE experiments (see Table 2 and Fig. 1). The meaningful NOE experiments performed on pseudo-petides **7**, **8**, **9**, **11** and **12**, in order to assign the amide protons $\mathbf{H^1}$, $\mathbf{H^2}$, $\mathbf{H^3}$ and $\mathbf{H^4}$, are collected in Table 2 and for clarity are depicted in Figure 1.

Inspection of the spectroscopic data of Table 1, usually employed to predict the propensity of single amide protons to form intra-molecular hydrogen bonds,[10] suggests some interesting observations. These data indicate that all the amide protons of the pseudo-peptides investigated here are involved in intra-molecular hydrogen bonds, except for $\mathbf{H^3}$ in substrate **11**. In this case the chemical shift value in $CDCl_3$ is significantly below 7 ppm and, more importantly, the singlet of the $\mathbf{H^3}$ amide protons is characterized by a significant high shift (0.74 ppm) upon addition of 20% DMSO (Table 1). In addition, the IR spectrum shows a sharp absorption at 3434 cm^{-1}, attributable to the free amidic NH stretching.

It is interesting to note that the chemical shift of $\mathbf{H^3}$ amide protons decreases going from the masked pseudo-peptide **6** to **7** and **11**. This trend indicates that hydrogen-bond formation is disfavoured by the presence of methyl groups in the chain. In addition, this low shift of $\mathbf{H^3}$ suggests that the introduction of CH_3 at the stereogenic centre to give an (*R*)-configuration (see compound **7**) again allows the formation of hydrogen bonds, while CH_3 in (*S*)-configuration (see compound **11**) does not favour the hydrogen bond. Moreover, going from precursors **6**, **7** or **11** to the pseudo-peptides **8**, **9** or **12**, respectively, the chemical shift of the $\mathbf{H^3}$ amide protons shows a significant to remarkable high shift (0.48–2.16 ppm), indicating the formation of an internal hydrogen bond, which could be stronger in **12** than in either **9** or **8**. Thus, in this case it is reasonable to infer that the presence of a methyl group in an (*S*)-configuration favours the formation of the internal hydrogen bond (compare **12** with **9**). A similar trend can be observed for the $\mathbf{H^1}$ amide protons, which show an increasing and significantly high shift when going from **8** to **9** and **12**. This trend enforces the hypothesis that the presence of the methyl group favours the intra-molecular hydrogen-bond formation, particularly when the substituent is involved in an (*S*)-configuration (see compound **12**). We wish to remark that the high chemical shift values of $\mathbf{H^1}$ and $\mathbf{H^3}$ (8 and 8.5 ppm, respectively) in the pseudo-peptide **12** are indicative of intra-molecular hydrogen bonds, while temperature gradient values (higher than 2.6 ppb/T[10]) would suggest the existence of a dynamic equilibrium between a hydrogen-bonded and a non-hydrogen-bonded structure. We believe that, in spite of the experimental observation carried out for small peptides (either linear or cyclic), in the case of complex and highly organized structures temperature gradient values might be affected not only by the hydrogen-bond lengthening, but also by the thermal motions of the groups surrounding the amide protons. When the temperature increases, these motions might affect the local magnetic field (shielding effects) in the vicinity of the hydrogen-bonded proton (amide protons). In our opinion this hypothesis is enforced by the observed low shift upon the addition of 20% DMSO. In fact, the $\mathbf{H^1}$ and $\mathbf{H^3}$ protons in the pseudo-peptide **12** shift to 7.86 and 7.97 ppm, respectively, instead of showing a high shift, as usually observed when a hydrogen-bonded structure is destroyed by a competitive solvent.

Table 2. Meaningful NOE data for substrates **7**–**9**, **11** and **12**

	Proton irradiated	NOE registered on the proton underlined		
7	$=CH_2$ s at 4.96 ppm	$=C–C\underline{H}_2$ doublets at 2.54 and 3.14 ppm	$C\underline{H}_3–C–NH^2$ s at 1.49 ppm	
	NH^2 s at 6.89 ppm	$=C–C\underline{H}_2$ doublets at 2.54 and 3.14 ppm	$C\underline{H}_3–C–NH^2$ s at 1.49	$=C\underline{H}_2$ s at 4.96 ppm
8	NH^1 d at 7.22 ppm	$C\underline{H}–NH^1$ dd at 4.51 ppm	$C\underline{H}–NH^2$ m at 4.71 ppm	
	NH^3 d at 7.95 ppm	$C\underline{H}–NH^3$ dd at 4.45 ppm	$C\underline{H}_3–C–NH^4$ s at 1.64 ppm	
9	$=CH_2$ s at 5.02 ppm	$=C–C\underline{H}_2$ d at 2.50 ppm	$C\underline{H}_3–C–NH^2$ s at 1.58 ppm	
	NH^1 d at 7.63 ppm	$C\underline{H}–NH^1$ dd at 4.53 ppm	$C\underline{H}_3–C–NH^2$ s at 1.58 ppm	$C\underline{H}(CH_3)_2$ m at 2.25 ppm
	NH^2 s at 7.45 ppm	$=C\underline{H}_2$ s at 5.02 ppm	$C\underline{H}_3–C–NH^2$ s at 1.58 ppm	$=C–C\underline{H}_2$ doublets at 2.50 and 2.83 ppm
11	$=CH_2$ s at 4.77 ppm	$=C–C\underline{H}_2$ doublets at 2.50 and 3.03 ppm	$C\underline{H}_3–C–NH^2$ s at 1.66	
	NH^2 s at 7.08 ppm	$=C–C\underline{H}_2$ doublets at 2.50 and 3.03 ppm	$C\underline{H}_3–C–NH^2$ s at 1.66	
12	$=CH_2$ s at 4.80 ppm	$=C–C\underline{H}_2$ doublets at 2.31 and 3.09 ppm	$C\underline{H}_3–C–NH^2$ s at 1.72	
	NH^1 s at 8.0 ppm	$C\underline{H}–NH^1$ dd at 4.85 ppm	$=C–C\underline{H}_2$ d at 2.31 ppm	$C\underline{H}_3–C–NH^2$ s at 1.72 ppm
	NH^4 s at 7.76 ppm	$C\underline{H}_2–C–NH^4$ d at 2.51 ppm	$C\underline{H}_3–C–NH^4$ s at 1.71 ppm	$C\underline{H}_3–CONH^4$ s at 2.04 ppm

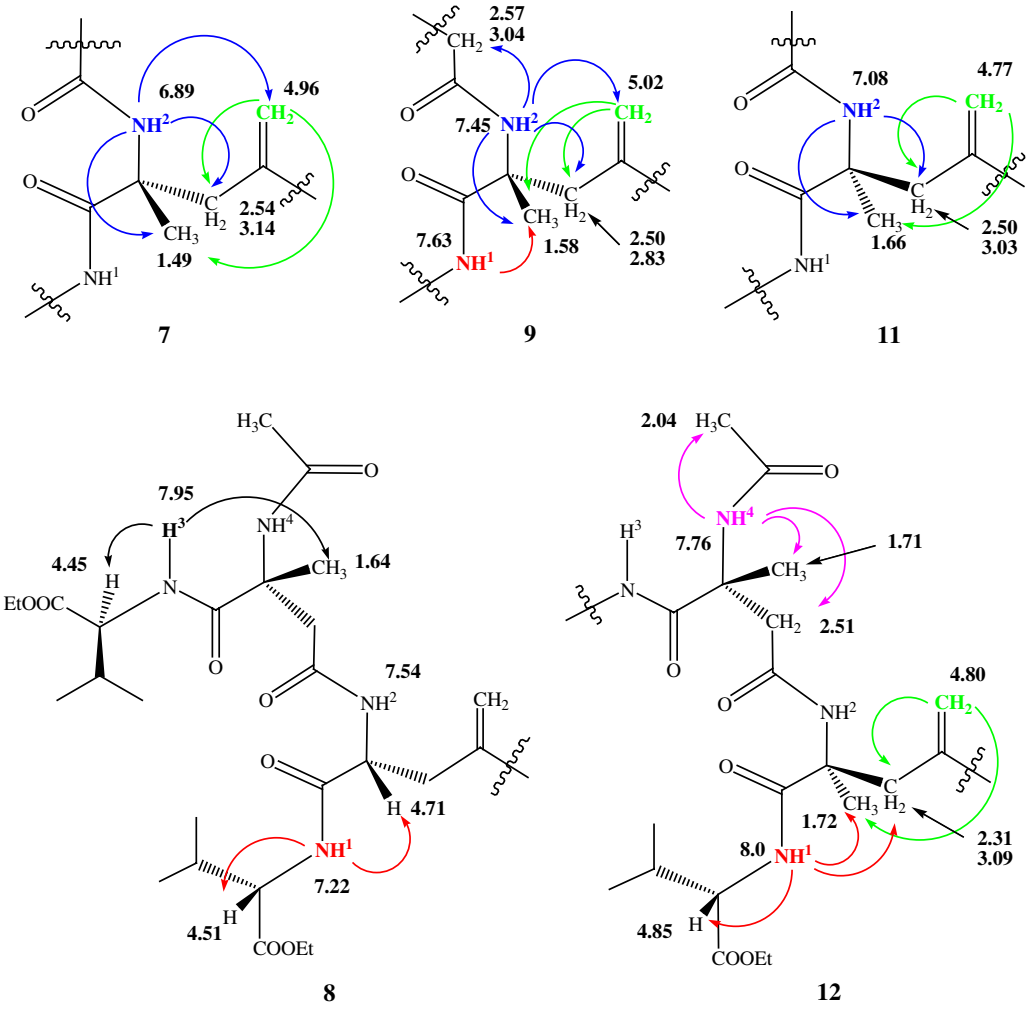

Figure 1. NOE experiments performed on **7**–**9**, **11** and **12**. Only the NOEs necessary to assign the amide protons are depicted (the chemical shift values are reported near the protons).

Finally, although the experimental data do not always allow us to come to a definitive conclusion on the presence of the intra-molecular hydrogen bond, we nevertheless believe that, on the basis of the significant temperature dependence value (6 ppb/°C) and the IR sharp band at 3404 cm^{-1}, the $\mathbf{H^3}$ proton in **6** is probably involved in a dynamic equilibrium between hydrogen-bonded and non-hydrogen-bonded structures. Besides, the IR spectra of **8** and **9** (meaning bands at 3420 and 3426 cm^{-1}, respectively) in connection to the temperature gradient values led us to suppose that the $\mathbf{H^1}$ proton is also involved in a similar dynamic equilibrium. Analogously to the $\mathbf{H^1}$ proton, we are inclined to believe that also $\mathbf{H^3}$ proton probably gives rise to a dynamic equilibrium in both **7** and in **12**.

4. Conformational analysis

The aim of the molecular dynamics (MD) simulation is the recognition of the hydrogen-bond pattern in the various pseudo-peptides examined here. This analysis is essential since the ^{1}H NMR can provide information on the existence of a given hydrogen bond, but cannot identify the acceptor involved in the interaction. The hydrogen bonds detected in precursors **6**, **7**, **11** and in the resulting pseudo-heptapeptides **8**, **9**, **12** are shown in Figures 2 and 3, respectively.

To verify the reliability of our simulation, we analyzed its capability of reproducing the C_2-symmetry axis suggested by the experimental data. This structural feature is evidenced in our analysis by the values of the lifetimes of the hydrogen bonds involving symmetry equivalent hydrogen atoms: for these hydrogen bonds, the mean difference between their lifetimes is only 1.6% (see Table 3).

The analysis of peptides **8**, **9**, **12** shows the same hydrogen-bond pattern: $\mathbf{H^1}\cdots O^2$, $\mathbf{H^2}\cdots O^3$, $\mathbf{H^3}\cdots O^4$, $\mathbf{H^4}\cdots O^2$. The most important hydrogen bond, which is responsible for the tri-dimensional structural features of the pseudo-peptides, is $\mathbf{H^1}\cdots O^2$. It is interesting to note that on passing from **8** to **9** and **12** [with the methyl substituent determining the configuration to be (*R*) or (*S*) at the stereocentre in **9** and **12**, respectively], the strength of this bond increases (the lifetime varies from 47% in **8** to 75% in **9** and 72% in **12**) and the corresponding structure becomes more sta-

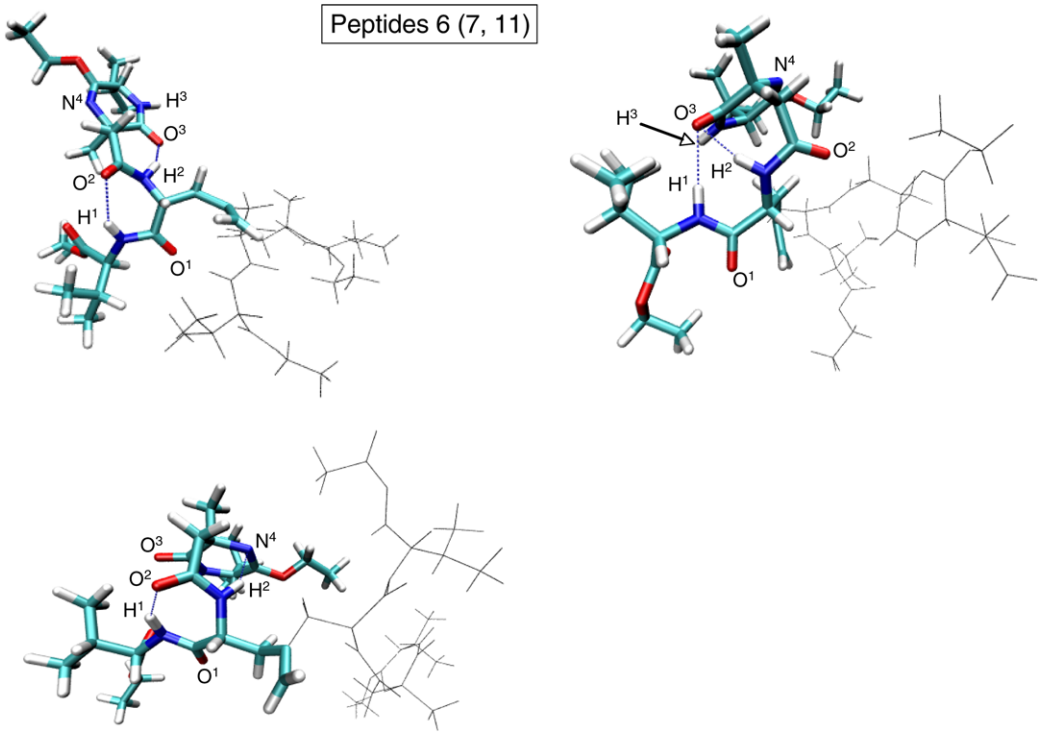

Figure 2. Snapshots taken from the MD simulation carried out for compound **6**. The hydrogen-bond patterns discussed in the paper are shown. A similar pattern has been obtained for peptides **7** and **11**. Due to the existence of a C_2-symmetry axis, only half the molecule is explicitly depicted.

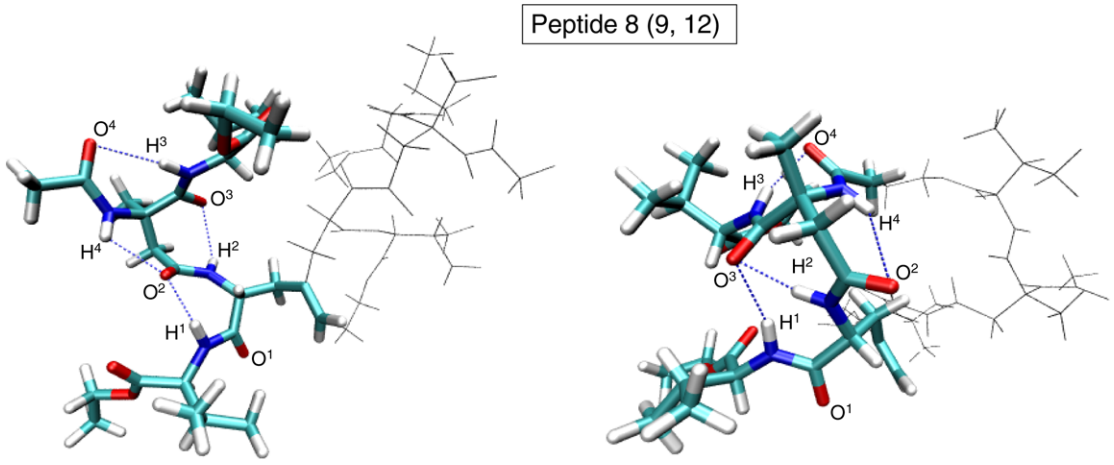

Figure 3. Snapshots taken from the MD simulation carried out for compound **8**. The hydrogen-bond patterns discussed in the paper are shown. A similar pattern has been obtained for peptides **9** and **12**. Due to the existence of a C_2-symmetry axis, only half the molecule is explicitly depicted.

ble. The increasing stability of the structure is due to the diminishing conformational freedom. It is possible to identify a different tri-dimensional structure where the seven-membered ring, held together by the $\mathbf{H^1}\cdots O^2$ interaction, is replaced by a 10-membered ring. For this larger cycle the important interaction is $\mathbf{H^1}\cdots O^3$ and this structural arrangement probably needs more flexibility. This hypothesis agrees with the results of our analysis, which show that after substitution of a hydrogen with a methyl group, the lifetime of $\mathbf{H^1}\cdots O^3$ decreases from 20% to 13% and 16%. The behaviour of pseudo-peptides **6**, **7** and **11** is very similar. Also in this case the lifetime of the $\mathbf{H^1}\cdots O^2$ bond, which determines the folded structure of the pseudo-peptides, increases from 44% to 75% and 76% after inclusion of the methyl substituent. Also, for these unnatural peptides, the formation of a 10-membered ring (held together by the $\mathbf{H^1}\cdots O^3$ interaction) is possible. However, in this case the lifetime of this hydrogen bond (15%) is not affected by the presence of the methyl substituent. This is probably due to the fact that pseudo-peptides **6**, **7** and **11** are less flexible and, thus, less sensitive to the hydrogen replacement in the case of a 10-membered cycle. On the contrary, the H/CH_3 substitution strongly affects the ability of $\mathbf{H^2}$ to form hydrogen bonds. In fact $\mathbf{H^2}$ in **6** interacts with O^3 and N^4 to the same extent (the corresponding lifetimes are 30% and 29%, respectively), while an (*R*)-substitution favours

Table 3. Lifetimes computed for the various hydrogen bonds in **6**–**9**, **11** and **12**

Pseudo-peptide	Hydrogen bond	Lifetime (%)
6	$\mathbf{H^1}$–O^2	44
	$\mathbf{H^2}$–O^3	30
	$\mathbf{H^2}$–N^4	29
	$\mathbf{H^1}$–O^3	15
7	$\mathbf{H^1}$–O^2	75
	$\mathbf{H^2}$–O^3	34
	$\mathbf{H^2}$–N^4	23
	$\mathbf{H^1}$–O^3	15
8	$\mathbf{H^3}$–O^4	70
	$\mathbf{H^1}$–O^2	47
	$\mathbf{H^4}$–O^2	44
	$\mathbf{H^2}$–O^3	38
	$\mathbf{H^1}$–O^3	20
	$\mathbf{H^3}$–O^2	17
9	$\mathbf{H^1}$–O^2	75
	$\mathbf{H^3}$–O^4	73
	$\mathbf{H^4}$–O^2	57
	$\mathbf{H^2}$–O^3	43
	$\mathbf{H^3}$–O^2	17
	$\mathbf{H^1}$–O^3	13
11	$\mathbf{H^1}$–O^2	76
	$\mathbf{H^2}$–N^4	38
	$\mathbf{H^2}$–O^3	19
	$\mathbf{H^1}$–O^3	15
12	$\mathbf{H^1}$–O^2	72
	$\mathbf{H^3}$–O^4	67
	$\mathbf{H^4}$–O^2	36
	$\mathbf{H^2}$–O^3	33
	$\mathbf{H^1}$–O^3	16

the $\mathbf{H^2}\cdots O^3$ interaction and an (*S*)-substitution favours the $\mathbf{H^2}\cdots N^4$ bond. For the (*R*)-configuration the lifetimes of $\mathbf{H^2}\cdots O^3$ and $\mathbf{H^2}\cdots N^4$ are 34% and 23%, respectively, while for the (*S*)-configuration we obtained 38% for $\mathbf{H^2}\cdots N^4$ and 19% for $\mathbf{H^2}\cdots O^3$. A possible explanation for this result is the strong effect of the substitution on the rotational equilibrium of the cycle.

5. Conclusions

New optically active pseudo-heptapeptides have been obtained in satisfactory overall yields starting from the chiral monolactim ether **1** and the chiral electrophile **2**. Both **1** and **2** are synthons that can be easily synthesized from L-valine. This approach represents a simple synthetic path for obtaining new peptidomimetic structures **8**, **9** and **12** containing four L-valine units, two modified aspartic acid units and the γ-methylene derivative of 2,6-diaminopimelic acid (2,6-DAP).

Spectroscopic investigations using ^{1}H NMR and IR techniques combined with a conformational analysis based on high-temperature molecular dynamics (MD) have been demonstrated to be a valid tool for elucidating the structures of these pseudo-peptides and the nature of intramolecular hydrogen bonds involving amide protons and carbonyl oxygen atoms. The MD analysis, based on the computed hydrogen bond lifetimes, agrees with the ^{1}H and ^{13}C NMR spectra suggesting the existence of a C_2-symmetry axis. The ^{1}H NMR and MD studies indicate that all the amide protons, except $\mathbf{H^3}$ in substrate **11**, are involved in intra-molecular hydrogen bonds. Pseudo-peptides **8**, **9** and **12** show an identical hydrogen-bond pattern where the most important role is played by $\mathbf{H^1}\cdots O^2$ that determines the structural features of these species (a seven-membered ring held together by the $\mathbf{H^1}\cdots O^2$ interaction). A similar behavior characterizes **6**, **7** and **11** with the $\mathbf{H^1}\cdots O^2$ hydrogen bond still determining the folded structures of these precursors. In all cases (**8**, **9**, **12** and precursors **6**, **7**, **11**), the $\mathbf{H^1}\cdots O^2$ bond lifetime increases after inclusion of a methyl substituent.

6. Experimental

6.1. General information

^{1}H and ^{13}C NMR spectra were recorded on a Gemini spectrometer at 300 MHz using $CDCl_3$ as the solvent, unless otherwise stated. Chemical shifts are reported in parts per million relative to $CDCl_3$ and the coupling constants (*J*) are in Hertz. IR spectra were recorded on a Nicolet 210 spectrometer. Optical rotations were measured at 25 °C on a Perkin–Elmer 343 polarimeter. Dry THF was distilled from sodium benzophenone ketyl. Chromatographic separations were performed with silica gel 60 (230–400 mesh).

Synthesis and spectroscopic data of compounds **1** and **3** are reported in Ref. 7b, while in Ref. 1 the data of compounds **4**, **5** and **10** are reported.

6.2. Pseudo-heptapeptide 6

Compound **4** (0.91 g, 2 mmol) was added to **3** (1.04 g, 4 mmol) dissolved in 15 mL of dry THF. After 10 min, DMTMM[8] (1.12 g, 4.8 mmol) was added and the reaction mixture stirred at room temperature for 12 h. The reaction mixture was filtered off and the solution diluted with ethyl acetate. The organic solution was washed first with 2 M NaOH and then quickly with 0.5 M HCl. After evaporation in vacuo to dryness, the residue was submitted to purification by silica gel chromatography eluting with hexane/ethyl acetate and the pure product was recovered as wax in 95% yield. ^{1}H NMR δ: 0.8–1.1 (m, 24H); 1.29 (t, 12H, $J = 7$); 1.5 (s, 6H); 2–2.5 (m, 8H); 2.57 (d, 2H, $J = 14.2$); 3.24 (d, 2H, $J = 14.2$); 4.03 (m, 2H); 4.18 (m, 8H); 4.47 (dd, 2H, $J = 5.2$, 8.8); 4.67 (m, 2H); 4.82 (br s, 2H); 7.47 (br s, 2H); 7.52 (d, 2H, $J = 8.8$); 7.74 (d, 2H, $J = 8.8$). ^{13}C NMR δ: 14.1, 16.2, 17.8, 18.4, 19.0, 29.5, 30.6, 30.9, 39.0, 47.2, 52.1, 57.1, 58.7, 59.0, 61.3, 113.0, 140.1, 156.7, 170.4, 172.7, 172.8, 174.0. $[\alpha]_D = -28$ (*c* 2.1, $CHCl_3$). Anal. Calcd for $C_{46}H_{70}N_2O_{12}$: C, 65.53; H, 8.37; N, 3.32. Found: C, 65.46; H, 8.39; N, 3.31.

6.3. Pseudo-heptapeptide 7

Compound **7** was prepared by reacting acid **3** (1.04 g, 4 mmol) with **5** (0.97 g, 2 mmol) and following the proce-

dure used for **6**. After purification by silica gel chromatography eluting with hexane/ethyl acetate, the pure product was recovered as a wax in 80% yield. ^{1}H NMR δ: 1 (m, 24H); 1.29 (t, 12H, $J = 6.6$); 1.49 (s, 12H); 2.16 (m, 2H); 2.3 (m, 2H); 2.54 (d, 2H, $J = 13.8$); 2.55 (q_{AB}, 2H, $J = 13.8$, 4); 3.14 (d, 2H, $J = 13.8$); 4.05 (m, 2H); 4.18 (m, 8H); 4.45 (dd, 2H, $J = 5.4$, 7.8); 4.96 (br s, 2H); 6.89 (s, 2H); 6.96 (br s, 2H); 7.59 (d, 2H, $J = 7.8$). ^{13}C NMR δ: 13.9, 14.0, 16.4, 17.9, 18.2, 18.9, 22.8, 29.0, 30.6, 30.8, 43.9, 48.2, 57.7, 58.7, 58.9, 59.7, 60.9, 61.3, 120.5, 138.9, 157.0, 170.3, 172.4, 173.9, 174.3. $[\alpha]_D = +10.2$ (c 1, $CHCl_3$). Anal. Calcd for $C_{48}H_{74}N_2O_{12}$: C, 66.18; H, 8.56; N, 3.22. Found: C, 66.42; H, 8.58; N, 3.21.

6.4. Pseudo-heptapeptide 8

A solution of HCl 0.5 M (4 mL) and **6** (0.42 g, 0.5 mmol) in ethanol (5 mL) was stirred at room temperature for 12 h. After evaporation in vacuo to dryness, CH_2Cl_2 (10 mL) and triethylamine (0.56 mL, 4 mmol) were added to the residue and the solution was cooled to −10 °C. Acetyl chloride (0.12 mL, 2 mmol) was then added and after 15 min the cooling bath was removed. The reaction mixture was stirred for about 3 h and the organic solvent evaporated under vacuum. The residue was dissolved in ethyl acetate, the organic solution washed with 2 M HCl and then dried over Na_2SO_4. After evaporation in vacuo to dryness, the residue was submitted to silica gel chromatography eluting with hexane/ethyl acetate. The pure product was recovered as a wax in 90% overall yield. ^{1}H NMR δ: 0.95 (m, 24H); 1.29 (t, 12H, $J = 6.6$); 1.64 (s, 6H); 2.06 (s, 6H); 2.22 (m, 4H); 2.48 (dd, 2H, $J = 8$, 15.4); 2.63 (dd, 2H, $J = 5.6$, 15.4); 2.72 (d, 2H, $J = 14.2$); 3.12 (d, 2H, $J = 14.2$); 4.2 (m, 8H); 4.45 (dd, 2H, $J = 4.8$, 8.4); 4.51 (dd, 2H, $J = 5$, 8.8); 4.71 (m, 2H); 4.88 (br s, 2H); 7.22 (d, 2H, $J = 8.8$); 7.54 (d, 2H, $J = 7.6$); 7.68 (s, 2H); 7.95 (d, 2H, $J = 8.4$). ^{13}C NMR δ: 14.1, 17.6, 17.7, 18.8, 23.1, 23.8, 30.9, 31, 37.8, 41.5, 51.2, 57.3, 57.5, 59, 61.1, 61.2, 116.1, 139.8, 171.2, 171.3, 171.6, 171.7, 171.8, 173.6. $[\alpha]_D = +67$ (c 0.7, $CHCl_3$). Anal. Calcd for $C_{50}H_{76}N_2O_{16}$: C, 62.48; H, 7.97; N, 2.91. Found: C, 62.69; H, 7.99; N, 2.92.

6.5. Pseudo-heptapeptide 9

Compound **9** was prepared from intermediate **7** and following the procedure used for **8**. After purification by silica gel chromatography eluting with hexane/ethyl acetate, the pure product was recovered as a wax in 90% yield. ^{1}H NMR δ: 0.98 (m, 24H); 1.29 (t, 12H, $J = 7$); 1.58 (s, 6H); 1.68 (s, 6H); 2.05 (s, 6H); 2.25 (m, 4H); 2.5 (d, 2H, $J = 14.2$); 2.57 (d, 2H, $J = 13.6$); 2.83 (d, 2H, $J = 14.2$); 3.04 (d, 2H, $J = 13.6$); 4.2 (m, 8H); 4.42 (dd, 2H, $J = 4.8$, 8.4); 4.53 (dd, 2H, $J = 5.2$, 8.4); 5.02 (br s, 2H); 7.45 (s, 2H); 7.58 (s, 2H); 7.63 (d, 2H, $J = 8.4$); 7.99 (d, 2H, $J = 8.4$). ^{13}C NMR δ: 14, 17.7, 18.9, 23.5, 23.9, 30.8, 31.2, 43.1, 57.3, 57.7, 59.1, 60.1, 60.9, 121.4, 139.9, 171, 171.3, 171.7, 172.1, 173.5, 173.7. $[\alpha]_D = +15.8$ (c 0.4, $CHCl_3$). Anal. Calcd for $C_{52}H_{80}N_2O_{16}$: C, 63.14; H, 8.15; N, 2.83. Found: C, 63.65; H, 8.18; N, 2.84.

6.6. Pseudo-heptapeptide 11

Compound **11** was prepared by reacting acid **3** with **10** and following the procedure used for **6**. After purification by silica gel chromatography eluting with hexane/ethyl acetate, the pure product was recovered as a wax in 65% yield. ^{1}H NMR δ: 0.89 (d, 6H, $J = 6.6$); 0.9 (d, 6H, $J = 6.6$); 0.96 (d, 6H, $J = 6.6$); 1.04 (d, 6H, $J = 6.6$); 1.29 (t, 6H, $J = 6.9$); 1.32 (t, 6H, $J = 6.9$); 1.42 (s, 6H); 1.66 (s, 6H); 2.28 (m, 4H); 2.29 (d, 2H, $J = 14.7$); 2.5 (d, 2H, $J = 14.7$); 3.03 (d, 4H, $J = 14.7$); 4.05 (m, 2H); 4.2 (m, 8H); 4.77 (br s, 2H); 4.8 (dd, 2H, $J = 5.1$, 9); 6.34 (br s, 2H); 7.08 (s, 2H); 7.79 (d, 2H, $J = 9$). ^{13}C NMR δ: 14, 14.1, 16.3, 17.3, 18.4, 19, 24, 29.6, 30.6, 31.3, 39.5, 40, 56.9, 58.4, 58.8, 60.3, 61.1, 61.6, 120.9, 137.6, 157.6, 169.1, 173.5, 173.9, 174. $[\alpha]_D = -10.6$ (c 1.5, $CHCl_3$). Anal. Calcd for $C_{48}H_{74}N_2O_{12}$: C, 66.18; H, 8.56; N, 3.22. Found: C, 65.9; H, 8.52; N, 3.24.

6.7. Pseudo-heptapeptide 12

Compound **12** was prepared from intermediate **11** and following the procedure used for **8**. After purification by silica gel chromatography eluting with hexane/ethyl acetate, the pure product was recovered as a wax in 90% yield. ^{1}H NMR δ: 0.98 (m, 24H); 1.29 (t, 6H, $J = 6.9$); 1.35 (t, 6H, $J = 7.2$); 1.71 (s, 6H); 1.72 (s, 6H); 2.04 (s, 6H); 2.25 (m, 4H); 2.31 (d, 2H, $J = 14.6$); 2.51 (d, 2H, $J = 14.8$); 3.07 (d, 2H, $J = 14.8$); 3.09 (d, 2H, $J = 14.6$); 4.2 (m, 8H); 4.43 (dd, 2H, $J = 4.5$, 8.1); 4.8 (br s, 2H); 4.85 (dd, 2H, $J = 3.9$, 9.6); 7.4 (s, 2H); 7.76 (s, 2H); 8 (d, 2H, $J = 9.6$); 8.5 (d, 2H, $J = 8.1$). ^{13}C NMR δ: 14, 14.1, 17.4, 19.1, 19.2, 22.8, 23.7, 24.2, 30.8, 31.2, 39.7, 42.9, 57.3, 57.7, 58.8, 60.5, 60.9, 61.9, 120.3, 138, 170, 170.6, 171.6, 173.5, 173.8. $[\alpha]_D = +36.2$ (c 0.6, $CHCl_3$). Anal. Calcd for $C_{52}H_{80}N_2O_{16}$: C, 63.14; H, 8.15; N, 2.83. Found: C, 63.24; H, 8.12; N, 2.82.

6.8. Computational details

The computational strategy used here is a high-temperature molecular dynamics (MD) approach,[11] which can provide reasonable molecular structures for a variety of pseudo-peptides. This MD protocol represents a powerful tool for investigating the conformational space and to locate the most populated conformations.

The 3D structures of the molecules were built with CORINA.[12] All calculations were performed at the molecular mechanics level using the AMBER 8.0 package.[13] Simulations were carried out using the Gaff force field.[14] Charges were assigned to atoms using the AM1-BCC method[15] as implemented in the Antechamber package.[16] Solvation effects were incorporated using the Generalized Born Model.[17] Thus, dynamics were performed with a dielectric constant $\varepsilon = 4.9$ to simulate the electrostatic effects of chloroform (the solvent in which ^{1}H NMR data have been recorded).

The high temperature MD needed to reproduce the C_2-symmetry axis must enable a statistically adequate sampling of the conformation space during the time of sim-

ulation, without being trapped in local minima. Thus, we first heated the molecules from 0 to 600 K in 100 ps and then, a trajectory of 50 ns was carried out at a constant temperature (600 K) and a constant pressure (1 atm) with an integration step of 2 fs. The SHAKE algorithm[18] was used to constrain the stretching of bonds involving hydrogen atoms. The coordinates of the pseudo-peptides investigated here were saved on a trajectory file every 1 ps, giving a total of 50,000 conformations for further analysis.

We analyzed this file with the 'PTRAJ' package (an AMBER module)[13] to obtain an estimate of the lifetime of the various hydrogen bond during the simulation. The lifetime is expressed as a percentage of the existence of the hydrogen-bonds during the whole simulation. These interactions must be characterized by a distance between the acceptor and the donor being shorter than 4 Å, and a bond angle larger than 90°.[19]

Acknowledgement

Thanks are due to the University of Bologna for the financial support ('Ricerca Fondamentale Orientata' ex 60%).

References

1. Balducci, D.; Crupi, S.; Galeazzi, R.; Piccinelli, F.; Porzi, G.; Sandri, S. *Tetrahedron: Asymmetry* **2005**, *16*, 1103, and references cited therein.
2. Balducci, D.; Emer, E.; Piccinelli, F.; Porzi, G.; Recanatini, M.; Sandri, S. *Tetrahedron: Asymmetry* **2005**, *16*, 3785, and references cited therein.
3. Balducci, D.; Grandi, A.; Porzi, G.; Sabatino, P.; Sandri, S. *Tetrahedron: Asymmetry* **2004**, *15*, 3929.
4. (a) Balducci, D.; Porzi, G.; Sandri, S. *Tetrahedron: Asymmetry* **2004**, *15*, 1085; (b) Paradisi, F.; Porzi, G.; Sandri, S. *Tetrahedron: Asymmetry* **2001**, *12*, 3319.
5. Balducci, D.; Bottoni, A.; Calvaresi, M.; Porzi, G.; Sandri, S. *Tetrahedron: Asymmetry* **2006**, *17*, 3273, and references cited therein.
6. (a) Paradisi, F.; Porzi, G.; Sandri, S. *Tetrahedron: Asymmetry* **2001**, *12*, 3319; (b) Galeazzi, R.; Garavelli, M.; Grandi, A.; Monari, M.; Porzi, G.; Sandri, S. *Tetrahedron: Asymmetry* **2003**, *14*, 2639.
7. (a) Balducci, D.; Grandi, A.; Porzi, G.; Sandri, S. *Tetrahedron: Asymmetry* **2006**, *17*, 1521; (b) Balducci, D.; Grandi, A.; Porzi, G.; Sandri, S. *Tetrahedron: Asymmetry* **2005**, *16*, 1453.
8. Kunishima, M.; Kawachi, C.; Morita, J.; Terao, K.; Iwasaki, F.; Tani, S. *Tetrahedron* **1999**, *55*, 13159.
9. (a) Cierpicki, T.; Otlewski, J. *J. Biomol. NMR* **2001**, *21*, 249, and references therein; (b) Andersen, N. H.; Neidigh, J. W.; Harris, S. M.; Lee, G. M.; Liu, Zhihong; Tong, Hui *J. Am. Chem. Soc.* **1997**, *119*, 8547; (c) Baxter, N. J.; Williamson, M. P. *J. Biomol. NMR* **1997**, *9*, 359.
10. (a) Baek, Bong-hyeon; Lee, Myung-ryul; Kim, Kwang-Yon; Cho, Ung-in; Boo, Doo Wan; Shin, Injae *Org. Lett.* **2003**, *5*, 971; (b) Trabocchi, A.; Occhiato, E. G.; Potenza, D.; Guarna, A. *J. Org. Chem.* **2002**, *67*, 7483; (c) Fernandez, M. M.; Diez, A.; Rubiralta, M.; Montenegro, E.; Casamitjana, N.; Kogan, M. J.; Giralt, E. *J. Org. Chem.* **2002**, *67*, 7587; (d) Yang, Dan; Li, Bing; Ng, Fei-Fu; Yan, Yi-Long; Qu, Jin; Wu, Yun-Dong *J. Org. Chem.* **2001**, *66*, 7303; (e) Belvisi, L.; Bernardi, A.; Manzoni, L.; Potenza, D.; Scolastico, C. *Eur. J. Org. Chem.* **2000**, 2563.
11. Carstens, H.; Renner, C.; Milbradt, A. G.; Moroder, L.; Tavan, P. *Biochemistry* **2005**, *44*, 4829.
12. Gasteiger, J.; Rudolph, C.; Sadowski, J. *Tetrahedron Comp. Method* **1990**, *3*, 537.
13. Case, D. A.; Darden, T. A.; Cheatham, T. E., III.; Simmerling, C. L.; Wang, J.; Duke, R. E.; Luo, R.; Merz, K. M.; Wang, B.; Pearlman, D. A.; Crowley, M.; Brozell, S.; Tsui, V.; Gohlke, H.; Mongan, J.; Hornak, V.; Cui, G.; Beroza, P.; Schafmeister, C.; Caldwell, J. W.; Ross, W. S.; Kollman, P. A. AMBER *8*; University of California: San Francisco, 2004.
14. Wang, J.; Wolf, R. M.; Caldwell, J. W.; Kollman, P. A.; Case, D. A. *J. Comput. Chem.* **2004**, *25*, 1157.
15. (a) Jakalian, A.; Bush, B. L.; Jack, D. B.; Bayly, C. I. *J. Comput. Chem.* **2000**, *21*, 132; (b) Jakalian, A.; David, B. J.; Bayly, C. I. *J. Comput. Chem.* **2002**, *23*, 1623.
16. Wang, J.; Wang, W.; Kollman, P. A.; Case, D. A. *J. Mol. Graphics Modell.* **2006**, *25*, 247.
17. (a) Hawkins, G. D.; Cramer, C. J.; Truhlar, D. G. *Chem. Phys. Lett.* **1995**, *246*, 122; (b) Hawkins, G. D.; Cramer, C. J.; Truhlar, D. G. *J. Phys. Chem.* **1996**, *100*, 19824.
18. Ryckaert, J.-P.; Ciccotti, G.; Berendsen, H. J. C. *J. Comput. Phys.* **1977**, *23*, 327.
19. (a) Peters, D.; Peters, J. *J. Mol. Struct.* **1980**, *68*, 255; (b) Baker, E. N.; Hubbard, R. E. *Prog. Biophys. Mol. Biol.* **1984**, *44*, 9; (c) Mitchell, J. B. O.; Price, S. L. *Chem. Phys. Lett.* **1989**, *154*, 267.